Thermal Characteristics and Crystallinity of Ziegler–Natta Isotactic Polypropylene/Metallocene Isotactic Polypropylene Polyblended Fibers

Yao-Chi Shu,[1] Kai-Jen Hsiao,[2] Wen-Chin Tsen[1]

[1]*Department of Polymer Materials, Vanung University, 1 Van Nung Road, Chungli City, Taiwan 320, Republic of China*
[2]*Division of Advanced Fiber and Bio Materials Research, Material and Chemical Research Laboratories, Industrial Technology Research Institute, Hsinchu, Taiwan 300, Republic of China*

Received 30 September 2007; accepted 29 July 2008
DOI 10.1002/app.30122
Published online 19 March 2009 in Wiley InterScience (www.interscience.wiley.com).

ABSTRACT: Ziegler–Natta isotactic polypropylene (ZN-iPP) and metallocene isotactic polypropylene (m-iPP) were extruded (in ratios of 75/25, 50/50, and 25/75) from one melt twin-screw extruder to produce three ZN-iPP/m-iPP polyblended polymers and, subsequently, spin fibers. In this study, we examined the rheology of the ZN-iPP/m-iPP polyblended polymers and the thermal characteristics and crystallinity of the ZN-iPP/m-iPP polyblended fibers using gel permeation chromatography, rheometry, differential scanning calorimetry (DSC), wide-angle X-ray diffraction, density gradient analysis, and extension stress–strain measurement. The apparent melt viscosity of the ZN-iPP/m-iPP polyblended polymers revealed positive-deviation blends. The 50/50 blend of ZN-iPP/m-iPP had the highest apparent melt viscosity. For five samples, the complex melt viscosity decreased with the angular frequency, which represented typical non-Newtonian behavior. The Cole–Cole plot, which consisted of the imaginary part of the complex melt viscosity versus the real part of the complex melt viscosity plot, of the ZN-iPP/m-iPP polyblended polymers showed a semicircular relationship with the blend ratios. It indicated that the ZN-iPP/m-iPP polyblended polymers were miscible. We analyzed the shear modulus data (G' vs G'') by plotting them on a log–log scale. The plot revealed almost the same slopes for the ZN-iPP/m-iPP polyblended polymers, which indicated a good miscibility between the ZN-iPP and m-iPP polymers. The experimental DSC results demonstrate that the ZN-iPP and m-iPP polymers constituted a miscible system. The crystallinity and tenacity of the ZN-iPP/m-iPP polyblended fibers initially increased and then fell as the m-iPP content increased. Meanwhile, the 50/50 blend of ZN-iPP/m-iPP had the highest crystallinity and tenacity. J Appl Polym Sci 113: 265–273, 2009

Key words: blends; fibers; miscibility; poly(propylene) (PP); thermal properties

INTRODUCTION

Thermoplastic alloys and blends have received widespread attention during the last several decades.[1–5] Polymer blending is an attractive alternative for the production of new polymeric materials with desirable properties without the synthesis of a totally new material. Other advantages of polymer blending are versatility, simplicity, and inexpensiveness. The purpose of blending polymers is to obtain materials with additional properties with minimum sacrifice of the original properties. Consequently, the applications of polyblends are important developments in the plastics and synthetic fiber industries. Polyblends are mixtures of two or more polymers that can either mix completely on a molecular scale or form a two-phase structure. Polyblends can exhibit new combinations of properties that depend on the properties of the components and strongly upon the morphology of the blended materials. The morphology resulting from a blending process depends mainly on the rheological and interfacial properties of the molten components, the blending conditions and the weight ratio of the polymers blended.[6–8] Polyblends can be characterized by their phase behavior as either miscible or immiscible. The thermal, mechanical, and rheological properties of a polyblend depend strongly on its state of miscibility.[9]

Polypropylene (PP) resins have been produced from Ziegler–Natta catalysts for over 50 years. These polymers are typically high-molecular-weight and broad-molecular-weight-distribution (MWD) resins as produced in the polymerization reactor. In recent years, these resins have frequently been given a postreactor treatment to a narrow their MWD and lower their molecular weight when they were to be used for fiber spinning. This treatment typically consists of extrusion in the presence of a peroxide

Correspondence to: K.-J. Hsiao (kjhsiao@itri.org.tw).

TABLE I
Synthetic Characteristics of the ZN-iPP and m-iPP Chips

Chip	MFR[a]	$\overline{M}_n$	$\overline{M}_w$	$\overline{M}_w/\overline{M}_n$[b]	T_m (°C)
ZN-iPP	32	86,000	187,000	2.17	166.2
m-iPP	32	72,000	138,000	1.92	149.6

$\overline{M}_n$ = number-average molecular weight.
[a] The MFR (g/10 min) values of the ZN-iPP and m-iPP polymers were measured from ASTM D 1238 method (230°C/2.16 kg).
[b] The MWDs of the ZN-iPP and m-iPP polymers were measured in a TCB solvent system.

compound, which produces the desired result by the thermal oxidative degradation of the reactor resin. This method is known as the *controlled rheology process.* A major advantage for the use of metallocene catalysts for the preparation of PP is that narrow-MWD resins can be obtained directly from the reactor without the need for secondary processing.[10]

There are also some reports on the physical properties of PP with other polymers, such as poly(ethylene terephthalate),[11] polyamide 6,[12–17] polyamide 12,[18] polyethylene,[19] and phenoxy.[20] The Ziegler–Natta isotactic polypropylene (ZN-iPP)/metallocene isotactic polypropylene (m-iPP) polyblended fiber is absent from the literature. In this study, both ZN-iPP and m-iPP belonged to polyolefin polymers and did not have any functional groups. Miscibility is essential in ZN-iPP/m-iPP polyblended fibers. This study thoroughly explores the thermal characteristics and crystallinity of the ZN-iPP/m-iPP polyblended fibers.

EXPERIMENTAL

Materials

Commercial-fiber-grade ZN-iPP chips were supplied by the Taiwan Polypropylene Co., Ltd. (Taipei, Taiwan). ZN-iPP (trade name PT232) had a melt flow rate (MFR) of 32 g/10 min and a melting temperature (T_m) of 166.2°C. m-iPP chips were obtained from the Exxon Chemical Taiwan (Taipei, Taiwan). m-iPP (trade name Achieve 3825) had a MFR of 32 g/10 min and a T_m of 149.6°C. Table I lists the synthetic characteristics of ZN-iPP and m-iPP chips. ZN-iPP and m-iPP were extruded (in ratios of 75/25, 50/50, and 25/75) from a Kobelco Hyperktx 30 twin-screw extruder (Kobe Steel, Ltd., Kobe, Japan) to prepare three ZN-iPP/m-iPP polyblended polymers. The extruder conditions were as follows: screw diameter = 30 mm, length-to diameter ratio (L/D) = 36.8, blending temperature = 260°C, blending time = 4.5 min, and screw speed = 60 rpm.

Melt spinning

Melt spinning was performed with a capillary spinner (AKS150) of Seiscor Technologies, Inc. (Tulsa OK); the L/D (2 : 0.4 mm) of the spinneret capillary was 5. Undrawn yarns (UDYs) were extruded at 260°C and at a constant wind speed of 300 m/min and were taken up for all samples. Then, the UDYs were drawn 3.5 times to produce fully drawn yarns (FDYs) by a drawn-winder machine (Diense, Berlin, Germany). The drawing temperature and take-up speed were 110°C and 50 m/min, respectively. The FDY was 33.3 dtex/10 filaments (3.33 dtex/f). Table II presents the compositions and mechanical properties of the ZN-iPP/m-iPP polyblended fibers.

Measurements

Gel permeation chromatography data were obtained with a Waters model 510 gel permeation chromatograph (Milford, MA). MWDs of the ZN-iPP and m-iPP polymers were measured in a 1,2,4-trichlorobenzene (TCB) solvent system. MFRs of both the ZN-iPP and m-iPP polymers were 32 g/10 min (ASTM D 1238 : 230°C/2.16 kg). The apparent melt viscosity and die swell ratio (D/D_0, where D and D_0 are the capillary diameter after and before the die swell of the melt polymer, respectively) of the samples were obtained with the AKS150 capillary rheometer, and the L/D (2 : 0.4 mm) of the capillary was 5.

Oscillatory rheological measurements were performed with a rotational rheometer (Gemini 200HR,

TABLE II
Compositions and Mechanical Properties of the ZN-iPP/m-iPP Polyblended Fibers

Polymer code	ZN-iPP/m-iPP blend ratio	UDY			FDY		
		Tenacity (cN/dtex)	Elongation (%)	Δn ($\times 10^{-3}$)	Tenacity (cN/dtex)	Elongation (%)	Δn ($\times 10^{-3}$)
Sample 1	100/0	1.18	352.1	12.2	4.02	34.2	40.3
Sample 2	75/25	1.43	338.1	16.6	4.66	32.1	44.2
Sample 3	50/50	1.81	328.1	18.2	4.98	30.5	45.6
Sample 4	25/75	1.72	333.7	17.3	4.85	31.4	44.8
Sample 5	0/100	1.36	345.4	16.3	4.64	33.2	43.9

Bohlin, United Kingdom) equipped with parallel plates 25 mm in diameter at 200°C and at frequency range from 0.01 to 100 rad/s. The storage modulus (G'), loss modulus (G''), and complex melt viscosity (η^*) were measured in the frequency sweep experiments. The real part of the complex melt viscosity (η') and the imaginary part of the complex melt viscosity (the η'') were calculated according to the following equation:

$$\eta' = G''/\omega$$

$$\eta'' = G'/\omega$$

$$\eta^* = \eta' - i\eta''$$

where ω is the angular frequency.[21,22]

Wide-angle X-ray diffraction (WAXD) studies of the samples were conducted with a MAC Science X-ray unit (Tokyo, Japan), which was operated at 35 kV and 30 mA. X-ray diffraction was then adopted with Cu Kα radiation and scanned from 5 to 25° (2θ) at a scan speed of 4°/min.[23–25] Differential scanning calorimetry (DSC) measurements of the samples were made with a PerkinElmer Pyrix-1 (Boston, MA). The heating and cooling rates in DSC measurement were 10°C/min between 30 and 200°C. The temperature was held for 3 min at 200°C. The crystallinity was calculated with the DSC method according to the following equation:

$$\text{Crystallinity}(\%) = \Delta H_m/\Delta H_m^o \times 100(\%)$$

where ΔH_m and ΔH_m^o are the heats of fusion (J/g) of the repeating units for the sample and at an ideal 100% crystallinity, respectively. The ΔH_m^o of pure PP is 209 J/g.[26]

The densities of the samples were determined with the density gradient method. A mixture of *n*-heptane and carbontetrachloride was used. The densities of the *n*-heptane and carbontetrachloride solvents were 0.684 and 1.595 g/cm^3, respectively. The density gradient method was implemented from 0.850 to 1.050 g/cm^3. All stress–strain data of the samples were obtained with a Zwick 1511 Instron instrument (Zwick, Bamberg, Germany) at an extension rate of 200 mm/min. The retardation of the optical path (Γ) of the polyblended fibers was measured with a Nikon Optical-Pol polarizing microscope and was measured by a compensator method. The wavelength was fixed to 546 nm. The birefringence (Δn) was calculated with the following equation:

$$\Delta n = \Gamma/d$$

where d is the thickness of the sample.[27,28]

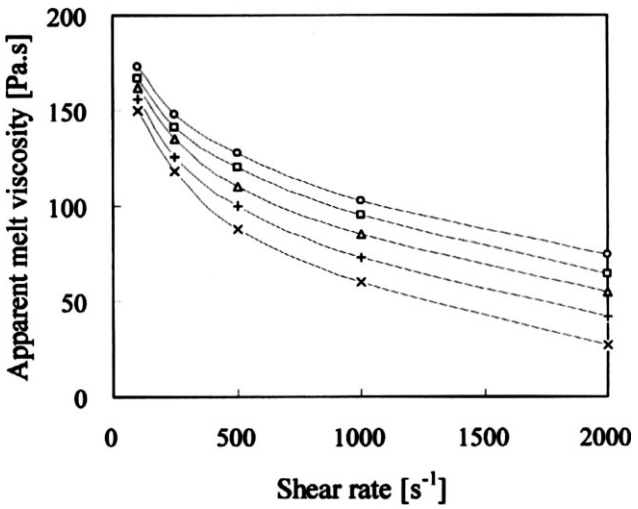

Figure 1 Apparent melt viscosity as a function of the shear rate for the ZN-iPP, m-iPP, and polyblended polymers at 260°C: (×) ZN-iPP/m-iPP (100/0), (△) ZN-iPP/m-iPP (75/25), (○) ZN-iPP/m-iPP (50/50), (□) ZN-iPP/m-iPP (25/75), and (+) ZN-iPP/m-iPP (0/100).

RESULTS AND DISCUSSION

Rheology of the polyblended polymers

The rheological properties of polyblended polymers depend strongly on their state of miscibility. The blend rheology of polyblended polymers depends on many variables, such as the blend ratio and melt viscosity of the homopolymers. Shear rate importantly influences the rheology of polyblended polymers. Figure 1 plots the apparent melt viscosities of the ZN-iPP, m-iPP, and polyblended polymers at 260°Cagainst shear rate. From 100 to 2000 s^{-1}, the five polymers exhibited pseudoplastic flow behavior. The flow curves indicated that the apparent melt viscosity of the m-iPP polymer exceeded that of the ZN-iPP polymer over the entire shear rate range. Fujiyama and Inata[29] reported that m-iPP showed a higher viscosity and weaker non-Newtonianity than ZN-iPP at an equivalent MFR. In addition, Cheng and Kuo[30] already reported that m-iPP displayed a smaller structural viscosity exponent and a weaker non-Newtonianity than ZN-iPP at an equivalent MFR. The apparent melt viscosities of the ZN-iPP/m-iPP polyblended polymers also revealed pseudoplastic flow behavior. This trend was independent of the blend ratio.

Figure 2 plots the apparent melt viscosities of the ZN-iPP/m-iPP polyblended polymers, which exhibited positive-deviation blends.[31–35] Notably, the 50/50 blend of ZN-iPP/m-iPP had a higher apparent melt viscosity than the value predicted by the additivity rule at 260°C/1000 s^{-1}. The apparent melt viscosities demonstrated good miscibility between the ZN-iPP and m-iPP polymers. The apparent melt viscosities of ZN-iPP, m-iPP, and their blends followed

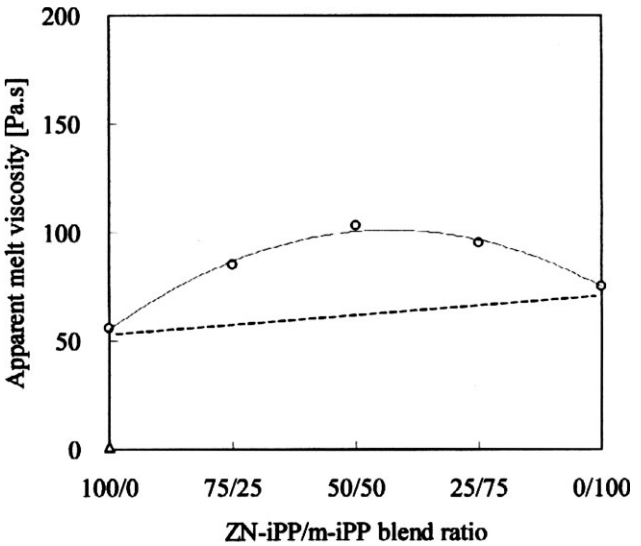

Figure 2 Apparent melt viscosity as a function of the blend ratio for the ZN-iPP/m-iPP polyblended polymers at 260°C/1000 s^{-1}.

the order ZN-iPP/m-iPP (50/50) > ZN-iPP/m-iPP (25/75) > ZN-iPP/m-iPP (75/25) > m-iPP > ZN-iPP.

Figure 3 shows the η* values of the ZN-iPP, m-iPP, and polyblended polymers at 200°C against ω.

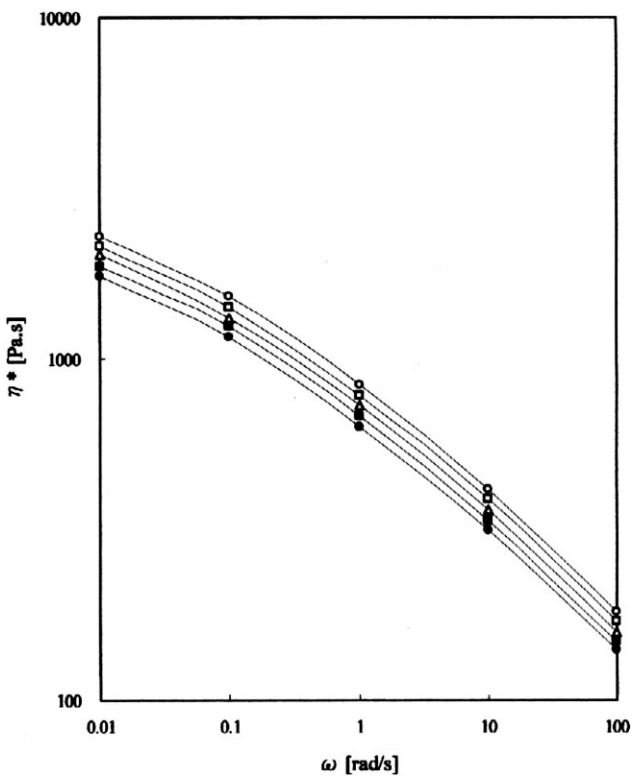

Figure 3 η* as a function of ω for the ZN-iPP, m-iPP, and polyblended polymers at 200°C: (●) ZN-iPP/m-iPP (100/0), (△) ZN-iPP/m-iPP (75/25), (○) ZN-iPP/m-iPP (50/50), (□) ZN-iPP/m-iPP (25/75), and (■) ZN-iPP/m-iPP (0/100).

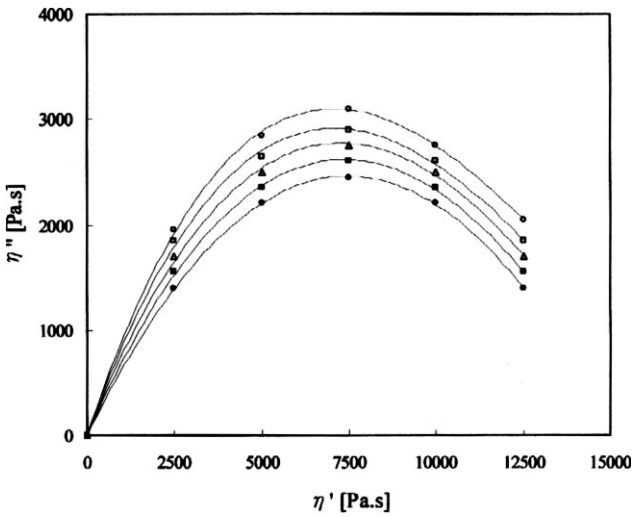

Figure 4 Cole–Cole plots (log η″ vs log η′) of the ZN-iPP, m-iPP, and polyblended polymers at 200°C: (●) ZN-iPP/m-iPP (100/0), (△) ZN-iPP/m-iPP (75/25), (○) ZN-iPP/m-iPP (50/50), (□) ZN-iPP/m-iPP (25/75), and (■) ZN-iPP/m-iPP (0/100).

For five samples, η* decreased with ω, which represented typical non-Newtonian behavior. Three different techniques were used to analyze the rheological data. The first technique was the Cole–Cole plot, which consisted of a η″ versus η′ plot. As shown in Figure 4, the ZN-iPP/m-iPP polyblended polymers showed a semicircular relationship with blend ratio. This indicated that the ZN-iPP/m-iPP polyblended polymers were miscible.[36] The second technique involved the shear modulus data (G' vs G''), which we analyzed by plotting them on a log–log scale.[37] As shown in Figure 5, the plot revealed almost the same slopes for the ZN-iPP/m-iPP polyblended polymers. This indicated a good miscibility between the ZN-iPP and m-iPP polymers. Miscibility in the molten state is related to both specific melt-phase interactions and miscibility in the solid state. The third technique, which was the plot of log η*, log η′, and log η″ as a function of the blend ratio, was used, and the representative plot of log η* versus blend ratio is depicted in Figure 6. The tendency of the plot of log η′ and log η″ versus blend ratio was similar to that shown in Figure 6. ZN-iPP and m-iPP exhibited a close linear relation from the log-additive rule. Under the assumption that there existed no specific interaction in the blends, the ZN-iPP and m-iPP blend was miscible. The miscibility in the melt state agreed well with that in the solid state.

D/D_0 of the polyblended polymers

Figure 7 plots the D/D_0 values of the ZN-iPP/m-iPP polyblended polymers at 260°C/1000 s^{-1} against

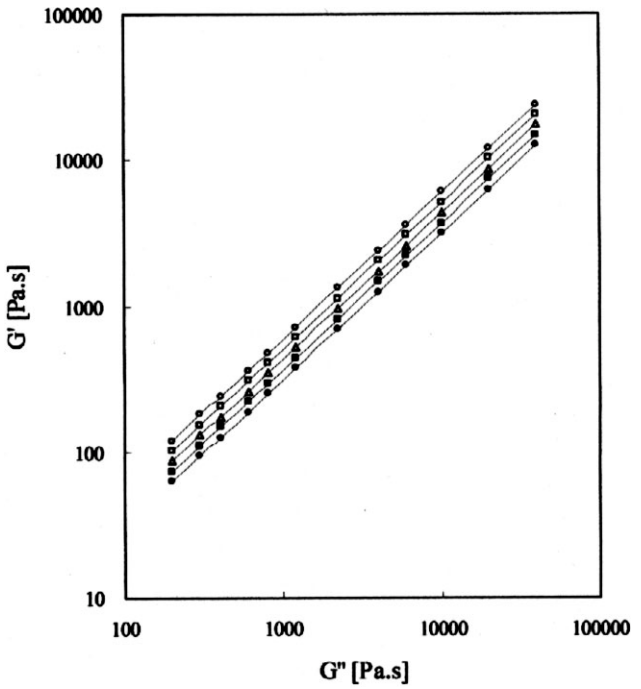

Figure 5 Han plots (log G' vs log G'') of the ZN-iPP, m-iPP, and polyblended polymers at 200°C: (●) ZN-iPP/m-iPP (100/0), (△) ZN-iPP/m-iPP (75/25), (○) ZN-iPP/m-iPP (50/50), (□) ZN-iPP/m-iPP (25/75), and (■) ZN-iPP/m-iPP (0/100).

shear rate. ZN-iPP, with a broader MWD, showed a higher D/D_0 than m-iPP. D/D_0 at a constant shear rate was higher, as the molecular weight was higher and the MWD was broader.[38,39] D/D_0 of the ZN-iPP/m-iPP polyblended polymers initially decreased and then increased as the m-iPP content increased. The 50/50 blend of ZN-iPP/m-iPP had a lower D/D_0. Figure 8 presents the weight-average molecular

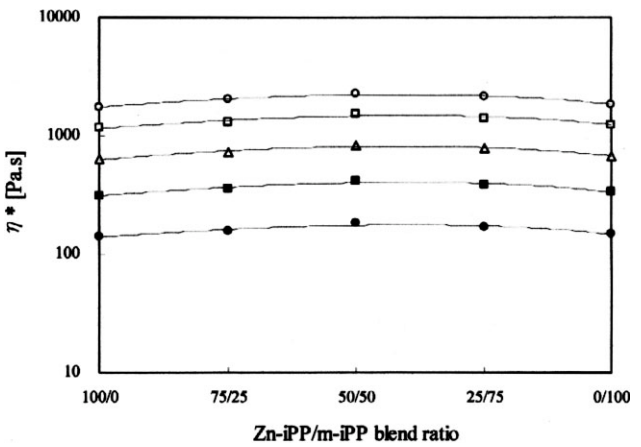

Figure 6 η* as a function of the blend ratio for the ZN-iPP, m-iPP, and polyblended polymers at 200°C: (●) ZN-iPP/m-iPP (100/0), (△) ZN-iPP/m-iPP (75/25), (○) ZN-iPP/m-iPP (50/50), (□) ZN-iPP/m-iPP (25/75), and (■) ZN-iPP/m-iPP (0/100).

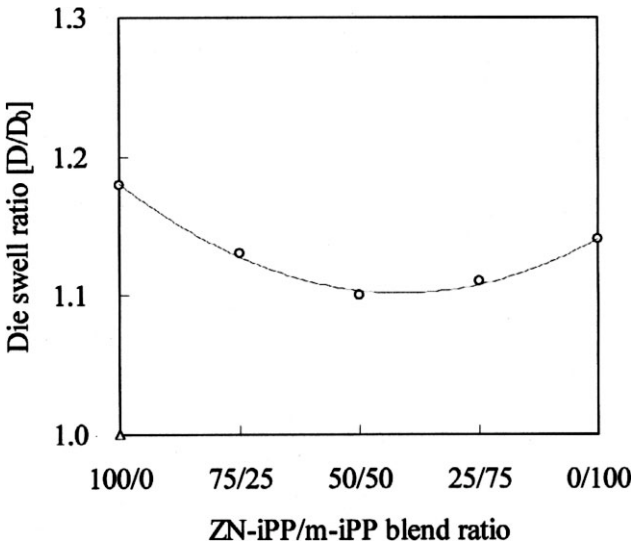

Figure 7 D/D_0 as a function of the blend ratio for the ZN-iPP/m-iPP polyblended polymers at 260°C/1000 s^{-1}.

weight ($\overline{M}_w$) and MWD as a function of blend ratio for the ZN-iPP/m-iPP polyblended polymers. $\overline{M}_w$ and MWD of the ZN-iPP/m-iPP polyblended polymers initially declined and then increased as the m-iPP content increased. The tendency of $\overline{M}_w$ and MWD resembled that of D/D_0 for the ZN-iPP/m-iPP polyblended polymers. Meanwhile, the 50/50 blend of ZN-iPP/m-iPP also had a lower $\overline{M}_w$ and MWD.

Thermal behavior of the polyblended fibers

Table III and Figure 9 display the thermal characteristics of ZN-iPP, m-iPP, and three ZN-iPP/m-iPP

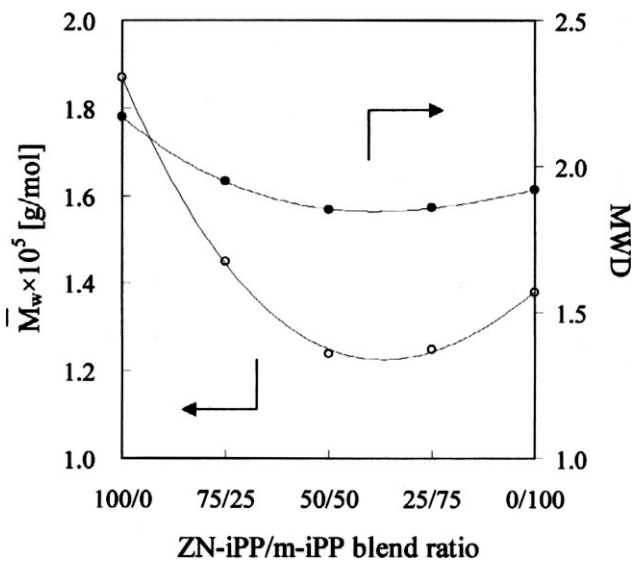

Figure 8 $\overline{M}_w$ and MWD as a function of the blend ratio for the ZN-iPP/m-iPP polyblended polymers: (○) $\overline{M}_w$ and (●) MWD.

TABLE III
Thermal Characteristics of the ZN-iPP, m-iPP, and ZN-iPP/m-iPP Polyblended Fibers

		Heating process			Cooling process		
Polymer code	ZN-iPP/m-iPP blend ratio	T_m (°C)	ΔH_m (J/g)	X_c (%)[a]	T_{cc} (°C)[b]	ΔH_{cc} (J/g)	X_{cc} (%)[c]
Sample 1	100/0	167.9	86.5	41.4	108.6	88.2	42.2
Sample 2	75/25	163.8	88.1	42.2	106.5	89.9	43.0
Sample 3	50/50	159.7	89.7	42.9	104.4	91.4	43.8
Sample 4	25/75	155.5	87.2	41.7	102.3	88.9	42.5
Sample 5	0/100	151.4	84.5	40.4	100.2	86.1	41.2

[a] Degree of crystallinity in heating process.
[b] The temperature of crystallinity in cooling process.
[c] Degree of crystallinity in cooling process.

polyblended fibers. In DSC heating, the endothermic peaks of the ZN-iPP and m-iPP fibers were obtained at 167.9 and 151.4°C, respectively. The endothermic peak (T_m) was associated with the melting of the sample. Tables I and III compare the T_m value of the ZN-iPP or m-iPP fiber with that of the ZN-iPP or m-iPP chip. The orientation and crystallization caused the T_m of the ZN-iPP or m-iPP fiber to clearly exceed that of the ZN-iPP or m-iPP chip. The T_m of the ZN-iPP fiber was higher than that of the m-iPP by approximately 16.5°C. This DSC data revealed a clear melting endothermic peak, which suggested that the ZN-iPP and m-iPP fibers were originally crystalline. For all of the ZN-iPP/m-iPP polyblended fibers, the DSC curves also demonstrated obviously melting endothermic peaks, which indicated that the ZN-iPP/m-iPP polyblended fibers were also crystalline materials, and the T_m of all samples was between 155 and 164°C. Meanwhile, the T_m of the ZN-iPP/m-iPP polyblended fibers declined as the m-iPP content increased.

During DSC cooling, the exothermic peaks (the T_{cc} points) of the ZN-iPP and m-iPP fibers were obtained at 108.6 and 100.2°C, respectively. The exothermic peak was associated with the crystallization of the melting polymer. Clearly, the T_{cc} of the ZN-iPP fiber was higher than that of the m-iPP fiber, which implied that the crystallization rate of the ZN-iPP fiber was faster than that of the m-iPP fiber. The T_{cc} of the ZN-iPP/m-iPP polyblended fibers appeared at 102–107°C. Both ΔH_m and the crystallization heat of the exothermic peak (ΔH_{cc}) fell as the m-iPP content increased. The DSC results indicate that the ZN-iPP and m-iPP crystallites were a miscible system.

Crystallinity and tenacity of the polyblended fibers

The crystallinities of the ZN-iPP, m-iPP, and ZN-iPP/m-iPP polyblended fibers were determined with the DSC, density gradient, and WAXD methods. In the DSC method, the heat of fusion was used to evaluate the crystalline fraction of the material. A higher heat of fusion was expected to correspond to a higher crystallinity. Table IV reveals the crystallinities of ZN-iPP, m-iPP, and their blends. The heat of fusion of the ZN-iPP/m-iPP polyblended fibers initially increased and then decreased as the m-iPP content increased, which indicated that the crystallinity initially increased and then fell. The data obtained by the DSC method were consistent with those obtained by the density gradient and WAXD methods.

The degree of crystallinity was compared from the DSC, density gradient, and WAXD measurements for all of the samples. According to the comparison,

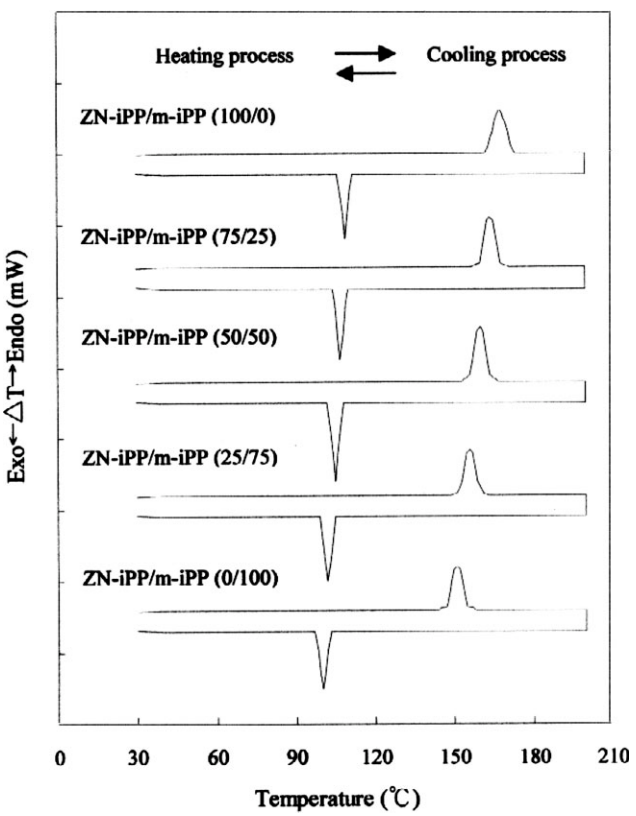

Figure 9 DSC curves of the ZN-iPP, m-iPP, and ZN-iPP/m-iPP polyblended fibers. ΔT, heat flow.

TABLE IV
Crystallinities of the ZN-iPP, m-iPP, and ZN-iPP/m-iPP Polyblended Fibers

Polymer code	ZN-iPP/m-iPP blend ratio	DSC		Density		WAXD
		ΔH_m (J/g)	X_c (%)[a]	d (g/cm^3)	X_c (%)[b]	X_c (%)[c]
Sample 1	100/0	86.5	41.4	0.8935	50.5	54.7
Sample 2	75/25	88.1	42.2	0.8943	51.4	55.6
Sample 3	50/50	89.7	42.9	0.8950	52.3	56.5
Sample 4	25/75	87.2	41.7	0.8941	51.2	55.4
Sample 5	0/100	84.5	40.4	0.8909	47.3	51.5

[a] Degree of crystallinity by DSC method.
[b] Degree of crystallinity by density gradient method.
[c] Degree of crystallinity by WAXD method.

quantifying the crystallinity by the DSC and density gradient methods was difficult. In the DSC analysis, ΔH_m was theoretically computed for 100% crystallinity of the PP polymer. With regard to the density gradient method, the density of the crystalline and amorphous PP polymers could not be measured accurately, and the literature values for the crystalline and amorphous density were assumed theoretically as well. Therefore, the crystallinity from the WAXD method was often used in the quantitative analysis of the crystallinity for the polymer.

Because the m-iPP polymer had a lower melt tension and elongational viscosity, m-iPP showed superior melt extensibility at melt spinning compared to ZN-iPP.[40] Clearly, Δn of m-iPP exceeded that of ZN-iPP (as shown in Table II). Figure 10 shows that the crystalline peak of the m-iPP fiber was slightly sharper than that of the ZN-iPP fiber. Three characteristic peaks of diffracting angles (2θ) for 14.0, 16.8, and 18.5°, corresponding to reflection planes of (110), (040), and (130) in equator direction, did not clearly shift as expected for the diffraction intensities. These peaks revealed the α form of isotactic PP (monoclinic structure).[41–52] The Δn values of the ZN-iPP/m-iPP polyblended fibers initially increased and then declined as the m-iPP content increased. The 50/50 blend of ZN-iPP/m-iPP had the highest Δn (as seen in Table II). The WAXD curves of the ZN-iPP/m-iPP polyblended fibers closely resembled those of the ZN-iPP and m-iPP fibers.

Figure 11 plots the crystallinity as a function of blend ratio for the ZN-iPP/m-iPP polyblended fibers. For all ZN-iPP/m-iPP polyblended fibers, the crystallinities initially increased and then decreased as the proportion of m-iPP increased. Obviously, the

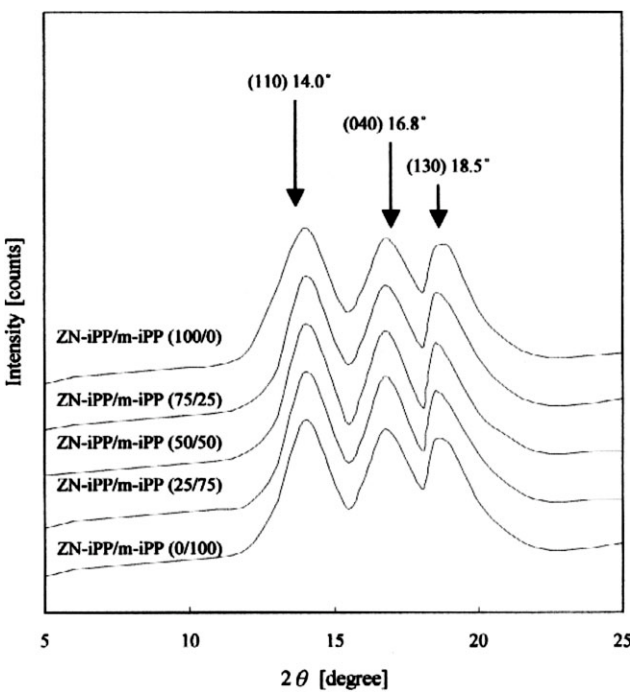

Figure 10 WAXD curves of the ZN-iPP, m-iPP, and ZN-iPP/m-iPP polyblended fibers.

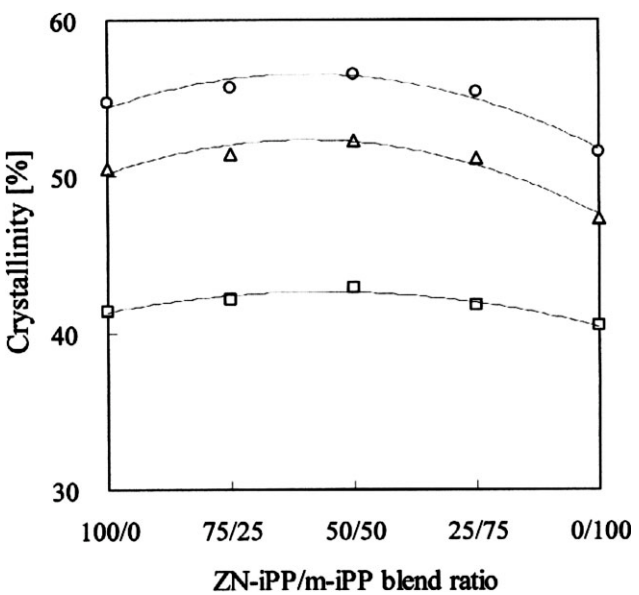

Figure 11 Crystallinity as a function of the blend ratio for the ZN-iPP/m-iPP polyblended fibers: (□) DSC, (△) density, and (○) WAXD methods.

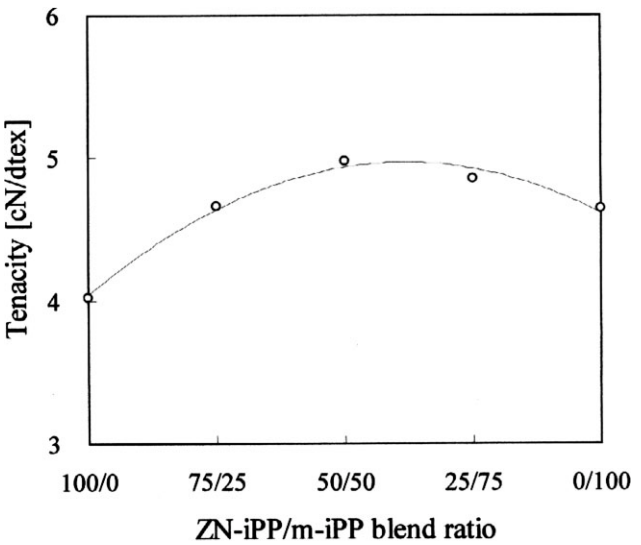

Figure 12 Tenacity as a function of the blend ratio for the ZN-iPP/m-iPP polyblended fibers.

50/50 blend ZN-iPP/m-iPP had the highest crystallinity. In this study, the crystallinities of the WAXD method were higher than those of DSC and density methods. Figure 12 plots the tenacity as a function of blend ratio for the ZN-iPP/m-iPP polyblended fibers. The tenacity of the ZN-iPP/m-iPP polyblended fibers initially also increased and then decreased as the m-iPP content increased. This result was consistent with the crystallinity and Δn. The good interfacial interactions between ZN-iPP and m-iPP demonstrated good mechanical properties. The aforementioned crystallinity, orientation, and miscibility of the ZN-iPP/m-iPP polyblended fibers and the trends of high crystallinity, high molecular orientation, and good miscibility increased the good mechanical properties.

CONCLUSIONS

The apparent melt viscosity of the ZN-iPP/m-iPP polyblended polymers was characteristic of positive-deviation blends. The 50/50 blend of ZN-iPP/m-iPP had a higher apparent melt viscosity than was predicted by the additivity rule. For five samples, η^* decreased with ω, which represented typical non-Newtonian behavior. The Cole–Cole plot, consisting of a η'' versus η' plot, of the ZN-iPP/m-iPP polyblended polymers showed a semicircular relationship with blend ratio. It indicated that ZN-iPP/m-iPP polyblended polymers were miscible. The shear modulus data (G' vs G'') revealed almost the same slopes for the ZN-iPP/m-iPP polyblended polymers, which indicated a good miscibility between the ZN-iPP and m-iPP polymers.

The experimental results of DSC reveal that the ZN-iPP and m-iPP polymers easily formed miscible domains. The crystallinity and tenacity of the ZN-iPP/m-iPP polyblended fibers initially increased and then fell as the m-iPP content increased. Meanwhile, the 50/50 blend of ZN-iPP/m-iPP had the highest crystallinity and tenacity. The rheology, thermal characteristics, crystallinity, and tenacity of the ZN-iPP/m-iPP polyblended fibers suggested that the ZN-iPP/m-iPP polymers were a miscible system.

References

1. Olabisi, O.; Robeson, L. M.; Shaw, M. T. Polymer–Polymer Miscibility; Academic: New York, 1979.
2. Han, C. D. Multiphase Flow in Polymer Processing; Academic: New York, 1981.
3. Cangelosi, F.; Shaw, M. T. Polymer Compatibility and Incompatibility: Principles and Practices; Solc, K., Ed.; MMI: New York, 1982.
4. Utracki, L. A. Polymer Alloys and Blends; Hanser: New York, 1989.
5. Utracki, L. A.; Shi, Z. H. Polym Eng Sci 1992, 32, 1824.
6. Vinogradov, G. V.; Yarlykov, B. V.; Tsebrenko, M. V.; Yudin, A. V.; Ablazova, T. I. Polymer 1975, 16, 609.
7. Ablazova, T. I.; Tsebrenko, M. V.; Yudin, A. V.; Vinogradov, G. V.; Yarlykov, B. V. J Appl Polym Sci 1975, 19, 1781.
8. White, J. L.; Plochoki. A. P.; Tanaka, H. Polym Eng Rev 1981, 1, 217.
9. Barlow, J. W.; Paul, D. R. Polym Eng Sci 1981, 21, 985.
10. Steinkamp, R. A.; Grail, T. J. U.S. Pat. 3,862,265 (1975).
11. Marcincin, A.; Ujhelyiova, A.; Marcincinova, T. Macromol Symp 2001, 176, 65.
12. Godshall, D.; White, C.; Wilkes, G. L. J Appl Polym Sci 2001, 80, 130.
13. Liang, B. R.; White, J. L.; Spruiell, J. E.; Goswami, B. C. J Appl Polym Sci 1983, 28, 2011.
14. Afshari, M.; Kotek, R.; Gupta, B. S.; Kish, M. H.; Dast, H. N. J Appl Polym Sci 2005, 97, 532.
15. Li, D.; Jia, D.; Zhou, P. J Appl Polym Sci 2004, 93, 420.
16. Afshari, M.; Kotek, R.; Kish, M. H.; Dast, H. N.; Gupta, B. S. Polymer 2002, 43, 1331.
17. Hornsby, P. R.; Tung, J. F. Plast Rubber Compos Process Appl 1991, 1, 16.
18. Jose, S.; Nair, S. V.; Thomas, S.; Karger-Kocsis, J. J Appl Polym Sci 2006, 99, 2640.
19. Li, J.; Shanks, R. A.; Long, Y. J Appl Polym Sci 2003, 87, 1179.
20. Choi, C. H.; Yoon, L. K.; Kim, B. K. J Appl Polym Sci 1996, 60, 779.
21. Cui, L.; Zhou, Z.; Zhang, Y.; Zhang, Y.; Zhang, X.; Zhou, W. J Appl Polym Sci 2007, 106, 811.
22. Zhou, Z.; Zhang, Y.; Zhang, Y.; Yin, N. J Polym Sci Part B: Polym Phys 2008, 46, 526.
23. Kunugi, T.; Suzuki, A.; Hashimoto, M. J Appl Polym Sci 1981, 26, 1951.
24. Hsiao, K. J.; Jen, Z. F.; Lu, C. L. J Appl Polym Sci 2002, 86, 3601.
25. Hsiao, K. J.; Jen, Z. F.; Yang, J. C.; Chen, L. T. J Polym Res 2002, 9, 53.
26. Godshall, D.; White, C.; Wilks, G. L. J Appl Polym Sci 2001, 80, 130.
27. Oh, T. H. J Appl Polym Sci 2006, 101, 1362.
28. Oh, T. H. J Appl Polym Sci 2006, 101, 1426.
29. Fujiyama, M.; Inata, H. J Appl Polym Sci 2002, 84, 2157.
30. Cheng, C. Y.; Kuo, J. W. J Plast Film Sheet 1999, 15, 82.

31. Utracki, L. A. Polym Eng Sci 1983, 23, 602.
32. Han, C. D.; Kim, Y. W. J Appl Polym Sci 1975, 19, 2831.
33. Kasajima, M. Bull Colloid Eng Hosei Univ 1979, 15, 1.
34. Shin, C. K. Polym Eng Sci 1976, 16, 742.
35. Patterson, D. D. Polym Eng Sci 1982, 22, 64.
36. Cole, K. S.; Cole, R. H. J Chem Phys 1941, 6, 341.
37. Han, C. D.; Kim, J. J Polym Sci Part B: Polym Phys 1987, 25, 1741.
38. Fujiyama, M.; Kitajima, Y.; Inata, H. J Appl Polym Sci 2002, 84, 2128.
39. Fujiyama, M.; Awaya, H. J Appl Polym Sci 1972, 16, 275.
40. Mori, K.; Saito, J. Seikei-Kakou 1996, 8, 649.
41. Galanti, A. V.; Mantell, C. L. Polypropylene Fibers and Films; Plenum: New York, 1965; p 6.
42. Ahmed, M. Polypropylene Fibres Science and Technology; Elsevier Scientific: Amsterdam, 1982; p 285.
43. Jin, Y.; Hiltner, A.; Bear, E.; Masirek, R.; Piorkowska, E.; Galeski, A. J Polym Sci Part B: Polym Phys 2006, 44, 1795.
44. Yuan, Q.; Jiang, W.; An, L.; Li, R. K. Y. J Polym Sci Part B: Polym Phys 2005, 43, 306.
45. Wang, Y.; Fu, Q.; Li, Q.; Zhang, G.; Shen, K.; Wang, Y. Z. J Polym Sci Part B: Polym Phys 2002, 40, 2086.
46. Wang, Z. G.; Phillips, R. A.; Hsiao, B. S. J Polym Sci Part B: Polym Phys 2001, 39, 1876.
47. Wu, G.; Wen, B.; Hou, S. Polym Int 2004, 53, 749.
48. Feng, J.; Chen, M. Polym Int 2003, 52, 42.
49. Naga, N. J Polym Sci Part B: Polym Phys 2004, 42, 1457.
50. Fan, Y.; Lou, J.; Shinozaki, D. M. J Appl Polym Sci 2007, 103, 204.
51. Wickoff, H. W. J Polym Sci 1962, 62, 83.
52. Morosoff, N.; Peterlin, A. J Polym Sci Part A-2: Polym Phys 1972, 10, 1237.